The Coherent EUV Scatterometry Microscope for Actinic Mask Inspection and Metrology

Tetsuo Harada*[1,3], Masato Nakasuji[1,3], Teruhiko Kimura[1,3], Yutaka Nagata[2,3], Takeo Watanabe[1,3], Hiroo Kinoshita[1,3]

[1] Center for EUV Lithography, Laboratory of Advanced Science and Technology for Industry, University of Hyogo, Kamigori, Hyogo 678-1205, Japan

[2] Core Research for Evolutional Science and Technology, Japan Science and Technology Agency, Kawaguchi, Saitama 332-0012, Japan

[3] Laser Technology Laboratory, RIKEN, Wako, Saitama 351-0198, Japan

ABSTRACT

For actinic mask inspection and metrology, we have developed a coherent EUV scatterometry microscope (CSM) at NewSUBARU of a synchrotron radiation facility. The CSM is composed of ϕ5-mm pinhole, turning and focusing multilayer mirrors, a test EUV mask and a back-illuminated CCD camera. Thus this system is lens-less system, records diffraction EUV light from a mask pattern, which is exposed with coherent EUV light. The CSM inspects defect on the EUV mask by the coherent-diffraction-imaging method. Aerial images of periodic and aperiodic patterns on the EUV mask were well reconstructed by the iterative calculation. Since the CSM data include only the diffraction intensity, the missing phase information is reconstructed. A defect with 10-nm width was well inspected.

The CSM also evaluates critical dimension (CD) of the mask patterns by diffraction intensities. The mask is illuminated with six-degree angle of the incidence, which equals to the EUV lithography scanners. The test EUV mask of 6025 glass substrate has line-and-space (L/S) patterns of 22-nm nodes. Absorber thickness is about 70 nm. The CSM result is well corresponding with the CD-SEM result at whole mask area. And, high repeatability of 0.3 nm (3σ) is achieved.

Keywords: EUV Lithography, Actinic inspection, actinic metrology, coherent EUV scatterometry microscope, lens-less imaging

1. INTRODUCTION

In extreme ultraviolet (EUV) lithography, the mask is of the reflective type composed of a glass substrate of 150 × 150 mm^2 in size, a Mo/Si multilayer, and absorber patterns. EUV mask fabrication has specific issues in EUV lithography such as phase defects of the multilayer and the shadowing effect due to the oblique illumination.[1-5] Thus, EUV inspection

* harada@lasti.u-hyogo.ac.jp; phone 81 791 58-2546; fax 81 791 58-2504; www.lasti.u-hyogo.ac.jp

Photomask and Next-Generation Lithography Mask Technology XVIII, edited by Toshio Konishi,
Proc. of SPIE Vol. 8081, 80810K · © 2011 SPIE · CCC code: 0277-786X/11/$18 · doi: 10.1117/12.896576

and metrology are required to evaluate the actinic feature of defect printability and critical dimension (CD) values.

There are two types of defects in EUV lithography masks: amplitude defects, which are caused by particles on the surface of a mask, and phase defects, which are caused by defects in the substrate and particles in the multilayer. To detect phase defects on mask blanks, SELETE has developed a dark-field inspection tool employing Schwarzschild optics and a laser plasma source.[6,7] To inspect finished (patterned) masks, the LBNL group developed an actinic inspection tool that employs a Fresnel zone plate as an optical component.[8,9] It is installed at the ALS synchrotron facility. This microscope has a numerical aperture (NA) of 0.0875, a field diameter of 5 μm and can estimate CDs ranging from 100 to 500 nm. However, aberration makes it difficult to obtain a high NA at the Fresnel zone plate. We have developed an EUV microscope that employs Schwarzschild optics and an x-ray zooming tube[10-12] and installed it at the NewSUBARU synchrotron facility. It has a high NA of 0.3 and a large field with a diameter of 50 μm. Because of the low magnification (30×) of the Schwarzschild optics, the zooming tube uses electromagnetic lenses to magnify a projected mask image by 10 – 200×. The optics for these actinic inspection tools is difficult to produce and align, and they become more complex as the NA and magnification become higher.

We have developed a coherent EUV scatterometry microscope (CSM), which is a lens-less system for actinic inspection and metrology.[13-14] For CSM, the mask is exposed to a coherent EUV light. A charge-coupled-device (CCD) camera records diffraction and scattering from the mask directly, which contains amplitude information in the frequency space. CD is estimated using diffraction intensity, and an aerial image of the pattern is reconstructed with iterative calculation. We observed line patterns and hole patterns, and the aerial images of these patterns were well reconstructed, and detected a program defect of 10-nm width. CD uniformity of a finished EUV mask was also evaluated.

2. DESIGN OF COHERENT SCATTEROMETRY MICROSCOPE

The CSM system has been installed at the BL-3 beamline of the NewSUBARU synchrotron radiation facility,[15] which employed a bending magnet as a light source. Two toroidal mirrors collimate the white light to the CSM system. Figures 1 and 2 show a photograph and a schematic view of the CSM system, respectively. A pinhole with a diameter of 5 μm is exposed to the collimated beam, which reduces the beam diameter. Then, a concave spherical mirror reflects the beam and a planar mirror reflects it onto an EUV mask. The concave mirror projects the pinhole image onto the mask. The radius of the curvature of the concave mirror is 160 mm, and distance from the pinhole to the concave mirror is 160 mm, which is the same as the distance from the concave mirror to the mask. The mirrors are coated with 40 pairs of Mo/Si multilayers. Diffractions from the mask are recorded with a back-illuminated CCD (Roper Scientific MTE-2048B) camera. This camera can operate in a high-vacuum environment. The CCD camera is cooled to a temperature of –50 °C. The surface of the CCD is placed parallel to the surface of the mask. The imaging area is 27.6 × 27.6 mm^2, which contains imaging pixels of 2048 × 2048 arrays with an area of 13.5 × 13.5 μm^2. The mask x-y stages can move ±75 mm through stepping motors to enable observation of the whole area of the EUV mask. The minimum step size of the stage is 100 nm. Two encoders of Magnescale LASERSCALE® of the noncontact optical type monitor the movements in the x-

and y-directions. The minimum signal step is 34.5 nm. The mask z stage can move 1.5 mm through a stepping motor to focus the exposure light on the mask.

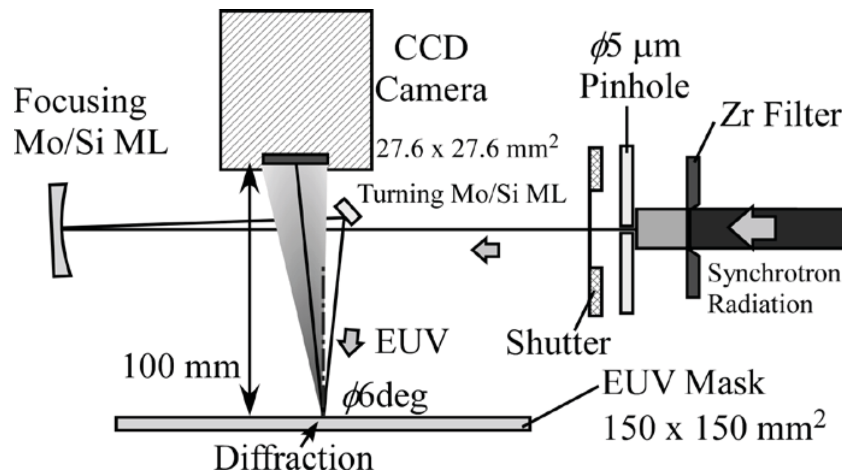

Fig. 1. Schematic view of the CSM system.

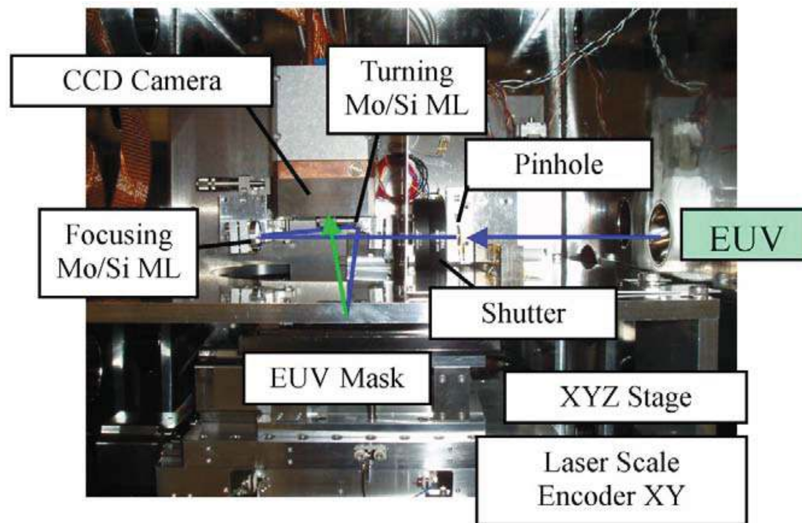

Fig. 2. Photograph of the CSM system. The arrows show the light path of synchrotron radiation. The CCD camera records diffraction from the EUV-mask pattern.

The angle of incidence on the EUV mask from normal is 6°, which is the same as those of the present EUV lithography scanners. Owing to the oblique illumination of the exposure tools, CD includes the shadowing effects caused by absorber pattern height. The shadowing effect causes a horizontal-vertical bias, which means a CD value difference between horizontal and vertical line-and-space (L/S) directions.[1] Thus, CSM can evaluate actinic CD value including the

shadowing effect. The spatial coherence length of the incident beam is 18 μm, as estimated from the divergence. This is substantially larger than the CSM-field size of 5 μm. The distance from the mask to the CCD camera is about 100 mm, which is equivalent to a numerical aperture of 0.14. The estimated spatial resolution is 50 nm at half pitch (hp). Figure 3 shows an example of a diffraction image recorded using the CCD camera. The sample was a L/S pattern with a 176 nm pitch. The center signal is directly reflected from the pattern of the 0th diffraction order, where diffraction fringes of Fraunhofer diffraction are recorded. The two signals besides the center are diffractions of ±1st order.

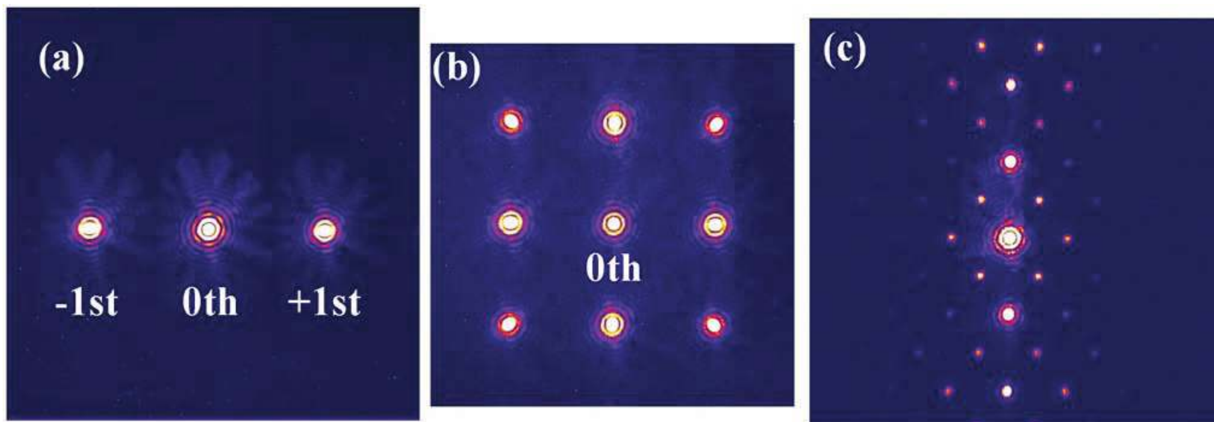

Fig. 3. Diffraction pattern images recorded with the CCD camera from (a) an L/S pattern with 176 nm pitch, (b) a hole pattern with 112 nm, and a bit-line pattern.

3. DEFECT INSPECTION

The sample EUV mask is a finished mask (Dai Nippon Printing), which is a glass substrate with 40 periods of the Mo/Si multilayer structure. The top layer of the multilayer is a 11-nm-thick silicon capping layer. The absorber is composed of a 10-nm-thick CrN layer (buffer layer) and a 70-nm-thick tantalum-based layer.

At CSM, the CCD camera records diffraction intensity from the patterns as shown in fig. 3, which contains amplitude information in frequency space. To reconstruct an aerial image, phase information is essential. However, the CCD camera cannot record the phase. This missing phase is retrieved by the coherent diffraction imaging method.[16-18] This method calculates iteratively the Fourier transform and the inverse Fourier, subject to constraints. Fig. 4 shows reconstructed aerial images by CSM. Fig 4(a) shows a reconstructed image of periodic pattern of 200-nm-hp hole. Periodic pattern of rectangular shape of the holes is well reconstructed. Fig. 4(b) shows that of an edge part of the periodic 128-nm L/S pattern. The periodic L/S structure and aperiodic edge structure are well reconstructed. Then CSM can observe EUV mask patterns as aerial image.

We also observed a program defect shown in fig. 5. An SEM image of this defect in 88-nm L/S pattern is shown in fig. 5(a). A single line of absorber has 30-nm narrower width than other lines. A diffraction intensity recorded by the CCD

camera is shown in fig. 5(b). Diffractions from the periodic structure are recorded as 0th and ±1st order, and diffraction from the defect is also recorded as line diffraction to lateral direction. Because the defect shape is line, the diffraction distribution is same as a slit diffraction. In this image, the line diffraction from the defect interfered with Fraunhofer diffraction rings around the 0th and ±1st order, because the illumination light was coherent. Thus, CSM can detect defect signal. At this CSM system, a 10-nm width defect was also detected clearly.

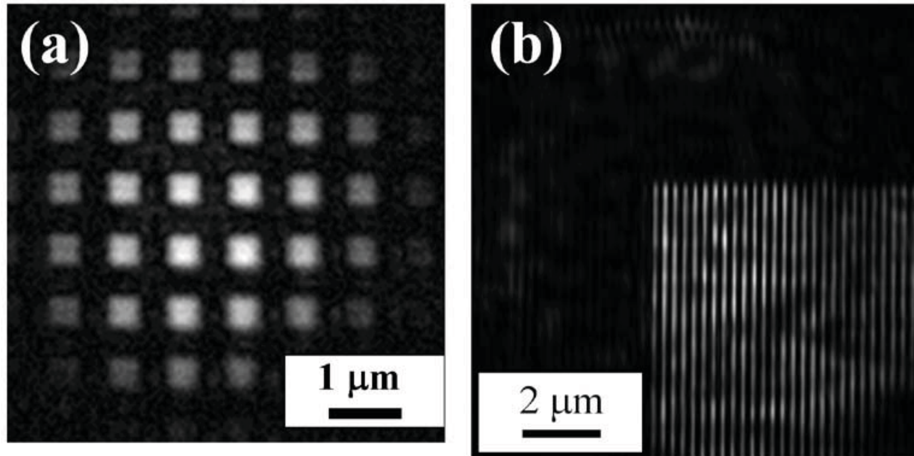

Fig. 4. Reconstructed images by CSM of (a) 200-nm hp hole pattern, and (b) edge part of a 128-nm hp L/S pattern.

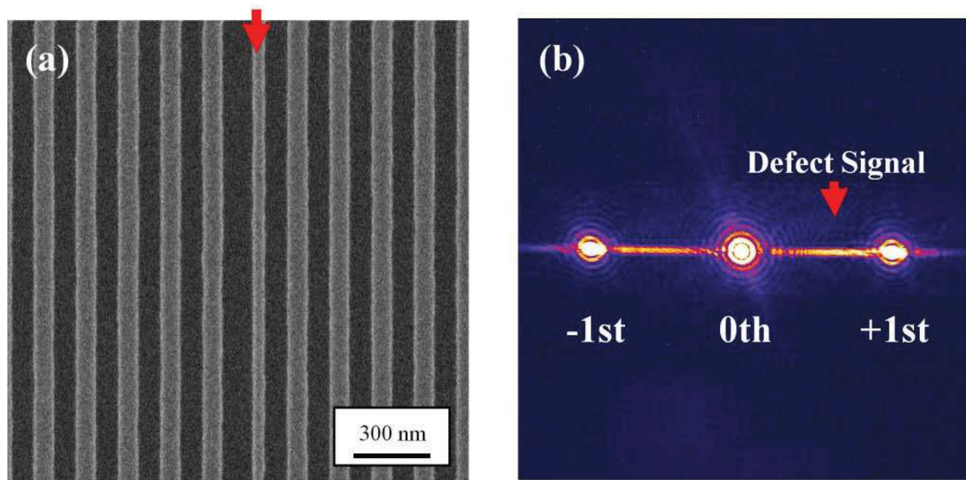

Fig. 5. (a) SEM image of the program defect in 88-nm L/S pattern. The line width is 30-nm narrow. (b) defect signal recorded by the CCD camera of CSM.

4. CD METROLOGY

We evaluated the image CD uniformity of the 10 × 9 patterns with 13 mm steps on a 150 × 150 mm^2 substrate. Each patterned area is 35 × 35 μm^2 of 88 nm L/S pattern. The distribution was also measured by CD-SEM (Vistec LWM9000), which has an average CD value of 91.9 nm and a uniformity of 7.7 nm (3σ). The magnification was 75,000×. The acceleration voltage was 1,500 V. The number of signal integrations was 128. The field of view was 1.9 × 1.9 μm^2.

The exposure time dependence of repeatability for 20 measurements is also shown in fig. 6, where the time is varied from 1 to 100 s. The repeatability is low at 2 nm (3σ) for 1 s, which is improved with increasing time; 0.3 nm for 20 s and 0.13 nm for 100 s. The image CD value is markedly stable even for different and long exposure times. We choose 20 s for evaluating image CD uniformity, considering the balance between exposure time and repeatability. The dark current noise of the CCD camera is about 0.02 electrons/s/pixel, and the readout noise is about 5.0 electrons/pixel at 100 Hz. Since the readout noise is dominant with less than 250 s of exposure time, the repeatability is limited by the signal-to-noise ratio of exposure dose and readout noise. Thus, the low repeatability of the short exposure time will be improved using a large dose. The high-brightness source of coherent EUV provides high-speed and high-precision measurement of image CD by CSM.

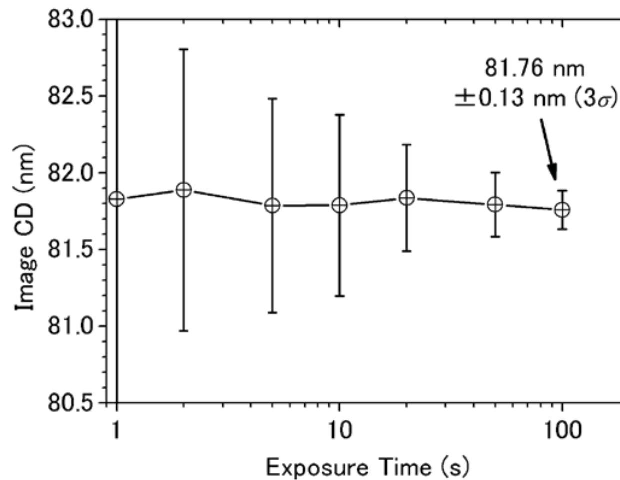

Fig. 6. Repeatability of CSM at various exposure times from 1 to 100 s. The error bar means the three-sigma deviation from the average.

The results of evaluation of image CD uniformity of the EUV mask are shown in Fig. 7. For this measurement, we did only position alignment to move the mask. Each square size shows the image CD value. The horizontal and the vertical axes indicate the x and y positions of the mask, respectively. The image CD values of the left side region are larger than

those of the right side. This distribution is almost the same as that of CD-SEM results. To compare with the CD-SEM results, the relationship between CSM and CD-SEM results is shown in Fig. 8. The vertical axis indicates the image CD value obtained by CSM, and the horizontal axis indicates the space width obtained by CD-SEM. Since the relationship is almost linear, CSM results correspond well to CD-SEM results. The deviation of CSM results from CD-SEM results is approximately 1.4 nm (3σ), which is comparable to the uncertainty of the CD-SEM results in this study. CSM can evaluate the actinic CD uniformity of the whole mask area with high speed and no complex alignment.

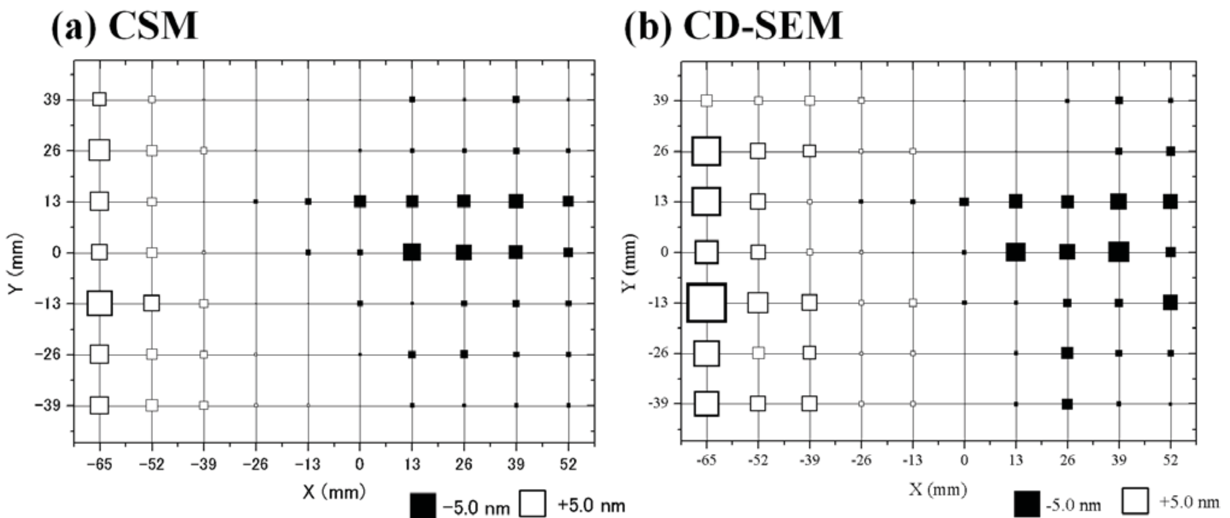

Fig. 7. Results of evaluation of image CD uniformity for (a) CSM, and (b) CD-SEM. The number of sampling points is 10 × 9, where the 88 nm L/S patterns fabricated by the same process are located with 13 mm steps.

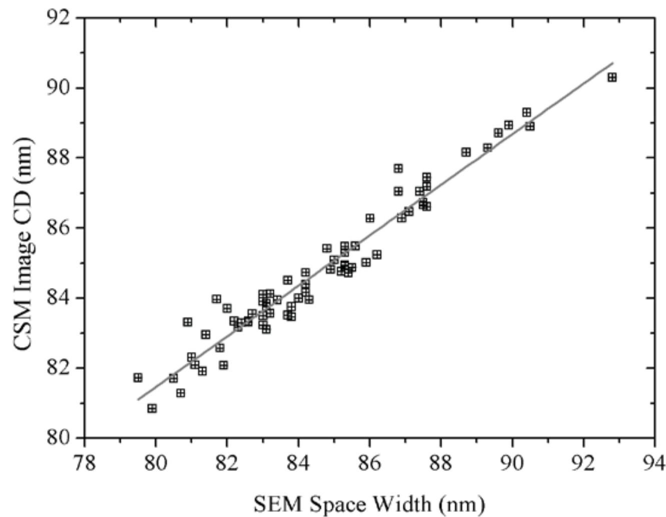

Fig. 7. CD value relationship measured using CSM and by CD-SEM of the EUV mask.

5. SUMMRY

We have developed the coherent EUV scatterometry microscope for actinic inspection and metrology of the EUV mask. The aerial images of 200-nm-hp hole structure and edge structure of 88-nm L/S structure were reconstructed with the diffraction intensity. And, 10-nm width program defect was well detected. The CD measurement method by estimation of the aerial image using the diffraction intensities has been developed. We evaluate the CD uniformity of the 88 nm L/S pattern with high repeatability of 0.3 nm (3σ), which corresponds well to that obtained by CD-SEM.

In the near future, we will install a laboratory EUV laser source of high-order harmonic generation (HHG) for practical inspection.[19] The power will be 1000 times greater than that of our present source, which wastes most of the light to achieve a high spatial coherence. The target scanning time for the whole mask is less than 90 min.

REFERENCES

1. K. Otaki: Jpn. J. Appl. Phys. **39** (2000) 6819.
2. T. Terasawa, T. Yamane, T. Tanaka, T. Iwasaki, O. Suga, and T. Tomie: Jpn. J. Appl. Phys. **48** (2009) 06FA04.
3. E. M. Gullikson, C. Cerjan, D. G. Stearns, P. B. Mirkarimi, and D. W. Sweeney: J. Vac. Sci. Technol. B **20** (2002) 81.
4. K. A. Goldberg, I. Mochi, and P. Naulleau: J. Vac. Sci. Technol. B **27** (2009) 2916.
5. Y. Kamaji, K. Takase, T. Yoshizumi, T. Sugiyama, T. Uno, T. Watanabe, and H. Kinoshita: Jpn. J. Appl. Phys. **48** (2009) 06FA07.
6. T. Terasawa, Y. Tezuka, M. Ito, and T. Tomie, Proc. SPIE **5446** (2004) 804.
7. T. Terasawa, T. Yamane, T. Tanaka, O. Suga, and T. Tomie: Jpn. J. Appl. Phys. **49** (2010) 06GD02.
8. A. Barty, Y. Liu, E. Gullikson, J. S. Taylor, and O. Wood, Proc. SPIE **5751** (2005) 651.
9. K. A. Goldberg, P. P. Naulleau, A. Barty, S. B. Rekawa, C. D. Kemp, R. F. Gunion, F. Salmassi, E. M. Gullikson, E. H. Anderson, and H. Han: Proc. SPIE **6730** (2007) 67305E.
10. T. Haga, H. Takenaka, and M. Fukuda: J. Vac. Sci. Technol. B **18** (2000) 2916.
11. K. Hamamoto, Y. Tanaka, T. Yoshizumi, N. Hosokawa, N. Sakaya, M. Hosoya, T. Shoki, T. Watanabe, and H. Kinoshita: Jpn. J. Appl. Phys. **45** (2006) 5378.
12. K. Takase, Y. Kamaji, N. Sakagami, T. Iguchi, M. Tada, Y. Yamaguchi, Y. Fukushima, T. Harada, T. Watanabe, and H. Kinoshita: Jpn. J. Appl. Phys. **49** (2010) 06GD07.
13. T. Harada, J. Kishimoto, T. Watanabe, H. Kinoshita, and D.G. Lee: J. Vac. Sci. Technol. B **27** (2009) 3203.
14. T. Harada, M. Nakasuji, M. Tada, Y. Nagata, T. Watanabe, and H. Kinoshita: Jpn. J. Appl Phys. (2011) Accepted.
15. T. Watanabe, T. Haga, M. Niibe, and H. Kinoshita: J. Synchrotron Rad. **5** (1998) 1149.

16. J. Miao, P. Charalambous, J. Kirz, and D. Sayre: Nature **400** (1999) 342.
17. J. Miao, Y. Nishino, Y. Kohmura, B. Johnson, C. Song, S. H. Risbud, and T. Ishikawa: Phys. Rev. Lett. **95** (2005) 085503.
18. J. R. Fienup: Appl. Opt. **21** (1982) 2758.
19. E. J. Takahashi, Y. Nabekawa, and K. Midorikawa: Appl. Phys. Lett. **84** (2004) 4.